

# Investigations of TiO<sub>2</sub> as a protective coating on diaphragm-based *in vivo* sensors

Ingelin Clausen, Trine M. Seeberg, Codin Gheorghe, Fabrice Prieur

**Abstract**—The motivation for these experiments has been to investigate the influence of a biocompatible protective coating on diaphragm-based *in vivo* sensors. The investigated device is a resonator for fish identification. Such a diaphragm-based configuration is also commonly used for pressure sensors. Six passive ID tags with a set of acoustic resonators have been coated with a 12 nm thin TiO<sub>2</sub> film by the atomic layer deposition (ALD) technique. The frequency response in the 200 kHz to 400 kHz range has been measured in water before and after coating. The resonance peaks can still be detected after coating, but an increase in the resonance frequencies of about 2 % is measured. The increase is explained by a thicker diaphragm due to the TiO<sub>2</sub> film.

## I. INTRODUCTION

Medical diagnostics and treatment is a rapidly developing application field for Micro Electro Mechanical Systems (MEMS). Small-sized, lightweight, and low power-consuming sensors open new avenues for monitoring of physiological parameters *inside* the human body. Research is in progress for several medical applications. A medicine pump inserted under the skin can control medicine flow for cancer patients who need pain relief and for patients with cerebral palsy [1]. Research is in progress on several implantable pressure sensors [2-5]. *In vivo* sensors are now being used for immediate inspection, or during surgery or for a short period after surgery. Except for one device, which will be left behind in the aneurism sac for possible post surgical pressure measurements, these devices are not meant for permanent implantation [6].

For permanent<sup>1</sup> implantation in the human body *biocompatibility* is one major obstacle for the success [7]. Biocompatibility comprises the impact of the sensor on the body (toxicity, inflammation, wear and degradation etc.) as

Manuscript received January 8, 2010. This work was supported in part by the University of Oslo, Department of Physics.

Ingelin Clausen is with SINTEF, Department of Microsystems and Nanotechnology, P.O Box 124, Blindern NO-0314 Oslo, Norway, (phone: +47 22067381; fax: +47 22067321; e-mail: [ingelin.clausen@sintef.no](mailto:ingelin.clausen@sintef.no)).

Trine M. Seeberg and Codin Gheorghe are with SINTEF, Department of Instrumentation, P.O Box 124, Blindern NO-0314 Oslo, Norway; (e-mail: [trine.seeberg@sintef.no](mailto:trine.seeberg@sintef.no)).

Fabrice Prieur is with University of Oslo, Department of informatics (e-mail: [fabrice@ifi.uio.no](mailto:fabrice@ifi.uio.no)).

<sup>1</sup> ISO 10993-1: devices whose single, multiple or long-term use or contact exceeds 30 days

well as the body's reaction to the implanted sensor (rejection, encapsulation, biofouling etc.) [8]. While the first aspect is paid attention to in several publications, the latter is seldom brought into focus. For sensors used *in vivo*, corrosion (caused by aggressive body fluids) as well as biofouling (accumulation of biological matter such as proteins, cells and other biological material), may alter the sensor characteristics. The sensor stability can be affected and sensor failure can be triggered. Research is in progress to minimize protein adsorption and cell adhesion in microfluidic devices or lab-on-a-chip systems [9, 10], but surprisingly little attention is given to biocompatible materials and their influence on *in vivo* sensors.

The use of a biocompatible protective coating can help reducing i) the microbially influenced corrosion and ii) the accumulation of proteins/cells on the sensor surface. However, a protective coating might affect the sensor characteristics dramatically. For thin diaphragm based devices e.g., a stiff coating might diminish the sensor sensitivity while a flexible coating might introduce hysteresis.

The objective of the work presented in this paper is to evaluate the influence of a protective biocompatible coating, i.e. TiO<sub>2</sub>, on a typical MEMS device. The investigated device is a diaphragm-based resonator for fish identification. Such a diaphragm-based configuration is also commonly used for pressure sensors.

## II. MATERIAL AND METHODS

### A. Resonators for fish identification

The MEMS device under investigation is a passive ID tag with a set of acoustic resonators [11]. The tag responds with a combination of specific resonance peaks to an interrogative ultrasound signal in the 200 kHz to 400 kHz range. The acoustic resonators are composed of five nominally 500 nm thick silicon nitride diaphragm suspended over separate evacuated cavities, anodic bonded to a glass wafer. The outer dimensions of the tag are about (length x width x height) 5 mm x 1.5 mm x 0.8 mm, and the diaphragms have quadratic form with side edge varying in size from 126 μm to 195 μm (Fig. 1).

The Si<sub>3</sub>N<sub>4</sub> film, with intrinsic stress of 300 MPa, was deposited by LPCVD on a 280 μm thick Si wafer. The resonator cavities were formed by backside TMAH etch followed by anodic bonding of a 500 μm thick glass wafer. A detailed description of the ID tags can be found in [12].

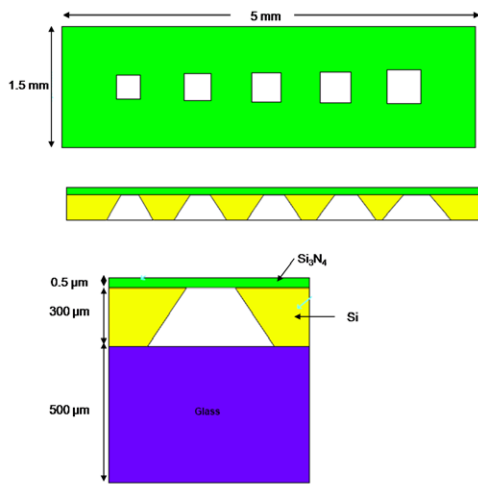


Fig. 1. Outline and side view of the passive ID tag with a set of five acoustic resonators (top). The acoustic resonators are composed of a silicon nitride diaphragm suspended over separate evacuated cavities, anodic bonded to a glass wafer (bottom) [12].

### B. Biocompatible coating

Titanium and titanium alloys are used in a wide variety of medical applications such as hip and knee prosthesis, pacemaker cages, internal fixation, stents, surgical devices, and for dental implants. The popularity of titanium-based materials for medical and dental implants is amongst other due to high strength, low density and a modulus of elasticity close to bone. Titanium is judged to be completely inert and immune to corrosion by all body fluids and tissue, and is thus wholly bio-compatible [13]. The good biocompatibility and corrosion resistance is explained by the native titanium oxide film [14].

In nature  $\text{TiO}_2$  occurs in three different crystallographic structures: rutile, anatase and brookite, but only anatase and rutile are made use of in applications [15]. Anatase can be synthesized at lower temperatures than rutile and may therefore be more attractive for MEMS devices, where high temperature processing may damage metallic lines and bond pads. For this reason anatase structure was chosen for the experiments presented here.

The  $\text{TiO}_2$  films were made by Baldur Coatings AS by the atomic layer deposition (ALD) technique using  $\text{TiCl}_4$  (99,9% Aldrich) and distilled water as precursors. Both precursors were supplied at room temperature, and the film was grown at 250 °C using a total of 60 cycles targeting in a thickness of 10 nm.

### C. Experimental set-up and measurement method

The experimental setup for the acoustical resonators is showed in Fig. 2 and listed below:

- a waveform generator Agilent model 33220A
- an oscilloscope Agilent model DOS6014A
- two transducers GE Panametric V1012
- a pre-amplifier set to 40dB amplification
- a water tank (l x w x h) 75cm x 75cm x 45cm

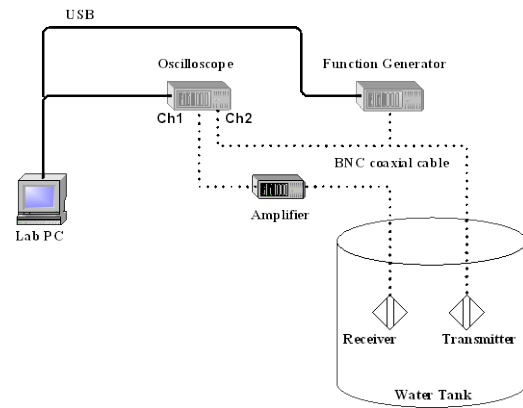


Fig. 2. Connection diagram for the used instruments

The temperature in the water was about 25°C. A positioning system in the water tank allowed accurate positioning of the transducers and the target. The fish tags were taped on a fish line held in place by two vertical poles and tested one by one. The poles were fixed far apart as not to disturb the acoustic field (Fig. 3).

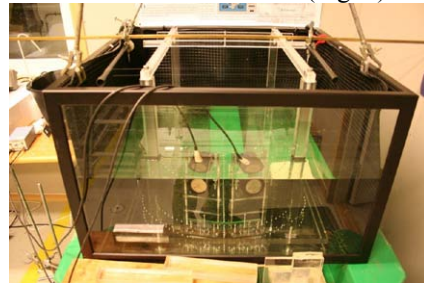


Fig. 3. Picture of the position system with the transmitter/receiver in the water tank.

The signal sent was a linear chirp varying from 150 kHz to 500 kHz as shown in Fig. 4 (left). Its frequency spectrum is relatively constant in the frequency domain of interest: 200 kHz to 400 kHz (Fig. 4, right). The frequency of the waveform generator was set to 7 kHz producing a chirp of duration 143 μs.

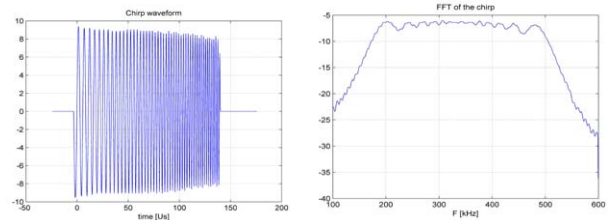


Fig. 4. Linear chirp from 150 kHz to 500 kHz are showed to the left and the frequency spectrum of the chirp is shown to the right.

A sensitivity study of the system revealed that the position of the received signal time window on the time-axis was a critical factor. This is the time window on which the Fourier transform of the received signal was calculated in order to get the frequency spectrum. The time delay, i.e. the time period between the triggering of the transmitter signal and the beginning of the receiver signal, was set to 320 μs. The time delay is given by the distance between transmitter/receiver and the position of the chip, and must be chosen in such a way that the important parts of the received signal fit into the time window for Fourier-transformation. Recorded signals for different delays (Fig. 5) and corresponding

frequency spectra (Fig. 6) clearly show that the spectrum is very sensitive to the time window.

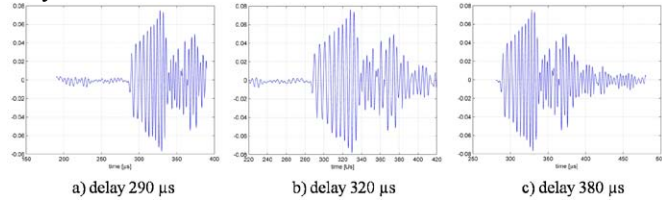


Fig. 5. Received signal with different time delay

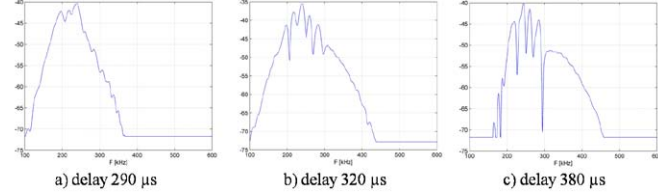


Fig. 6 Spectra with different time windows

To minimize the error in the reproducibility of the measurement this procedure was followed: The fish tags were first inserted into the position system in the aquarium and the resonance frequency was measured. Then the sample was taken out and reinserted. The above were repeated 3-5 times for each sample. The average of all 3-5 spectra was plotted and the peak for each resonance frequency was manually found.

### III. RESULTS AND DISCUSSIONS

Six tags (TiO<sub>2</sub>-A to TiO<sub>2</sub>-F) were coated with TiO<sub>2</sub>. The final film thickness was measured to ~ 12 nm by ellipsometry (Fig. 7).

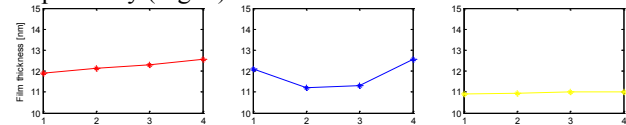


Fig. 7. Film thickness of TiO<sub>2</sub> measured on three Si control samples of size 7 mm x 7 mm by ellipsometer.

The frequency response of each tag was measured before and after coating. In addition three uncoated tags were measured to serve as control samples (CTRL-A to CTRL-C). An example of the measured frequency response is given in Fig. 8. In Fig. 9 the resonance frequencies are interpreted. The different peaks correspond to the acoustic resonators outlined in Fig. 1. Peak 1 corresponds to the resonator to the right and peak 5 corresponds to the resonator to the left.

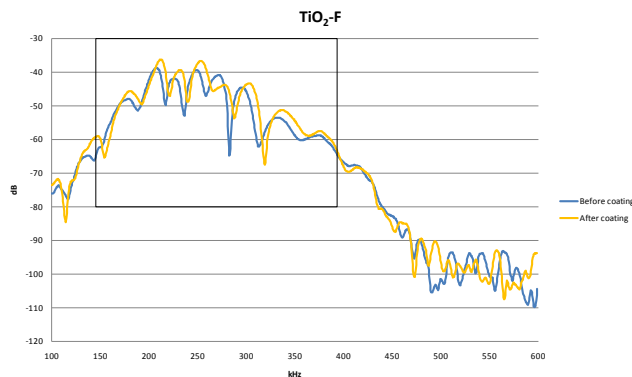


Fig. 8. An example of the frequency response before and after coating (sample TiO<sub>2</sub>-F). The blue curve is the spectrum before coating and the yellow curve is the spectrum after coating.

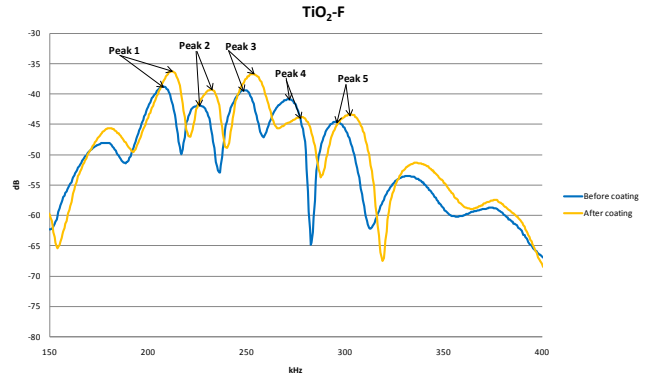


Fig. 9. Example of the interpretation of the frequency resonances. Only parts of the frequency spectrum of the TiO<sub>2</sub>-F are showed. The different peaks correspond to the acoustic resonators outlined in Fig. 1.

TABLE I shows the theoretical and the measured values for the resonance frequency for all samples. The uncertainty in the interpretation of the peaks is estimated to  $\pm \sim 2$  kHz.

TABLE I  
RESONANCE FREQUENCY [KHZ] BEFORE AND AFTER COATING OF THE FISH TAGS WITH TiO<sub>2</sub>. UNCERTAINTY  $\sim 2$  KHZ.

Sample name	Peak 1 [kHz]	Peak 2 [kHz]	Peak 3 [kHz]	Peak 4 [kHz]	Peak 5 [kHz]
Theoretical value	200	218	238	259	283
TiO <sub>2</sub> -A Pre	201	220	244	261	284
TiO <sub>2</sub> -A Post	206	224	248	265	291
TiO <sub>2</sub> -B Pre	202	220	240	259	289
TiO <sub>2</sub> -B Post	206	224	248	264	294
TiO <sub>2</sub> -C Pre	204	221	240	263	287
TiO <sub>2</sub> -C Post	207	225	246	266	293
TiO <sub>2</sub> -D Pre	202	221	242	264	290
TiO <sub>2</sub> -D Post	206	225	248	267	296
TiO <sub>2</sub> -E Pre	202	221	244	264	288
TiO <sub>2</sub> -E Post	206	225	247	269	295
TiO <sub>2</sub> -F Pre	205	226	247	270	294
TiO <sub>2</sub> -F Post	211	231	251	274	300
CTRL-A Pre	198	217	240	255	278
CTRL-A Post	198	217	238	256	277
CTRL-B Pre	201	218	244	261	289
CTRL-B Post	202	220	244	261	286
CTRL-C Pre	201	221	244	263	291
CTRL-C Post	203	223	244	263	289

In Fig. 10 the relative shift in resonance frequencies as a function of coating is given. The value on the y-axis (and in the table) is given by the formula below.

$$\frac{\Delta f}{f} \times 100\%$$

$\Delta f$  is the shift in frequency, and  $f$  is the resonance frequency before coating. The resonance frequencies increase about 4-6 kHz for coated samples.

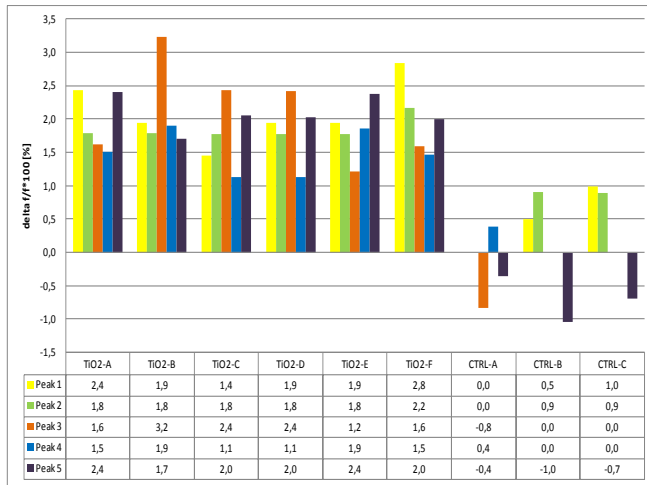


Fig. 10. Relative shift in resonance frequencies for each resonator as a function of coating (after coating - before coating) for six samples coated with TiO<sub>2</sub> (TiO<sub>2</sub>-A to TiO<sub>2</sub>-F) and three uncoated control samples (CTRL-A, -B and -C). The value on the y-axis (and in the table) are  $(\Delta f/f) \cdot 100\%$ . Each resonator (peak) is given an individual color code.

The observed changes in resonance frequency were as expected. When the diaphragm is small compared to the wavelength, the resonance frequency is given by

$$f = \frac{1}{2\pi} \sqrt{\frac{k}{m}} = \frac{1}{2\pi} \sqrt{\frac{k}{m_d + m_w}}$$

where  $k$  is the spring constant and  $m$  the mass of the diaphragm. Two limit cases exist; one for thin diaphragms where  $k \propto \sigma$  ( $\sigma$  is tension due to in-plane stress,  $t$  is thickness), the other for thicker diaphragms where  $k \propto D$  ( $D$  is the flexural rigidity and goes as  $t^3$ ) [16]. In air we can consider the acoustic resonators to be composed of thin diaphragms of mass  $m_d$ . A change in thickness due to the TiO<sub>2</sub> coating would alter  $m_d$  and  $k$  equally, and the resonance frequency would depend only on the tension. However, for our measurements there is an additional and constant mass  $m_w$  due to the water. This mass completely dominates  $m_d$  and  $k$  will therefore increase with  $t$  no matter if the diaphragm is tension-dominated (thin diaphragm) or flexural rigidity-dominated (thicker diaphragm). An increase in the resonance frequency due to an increased thickness of the diaphragm will follow.

Several sources of errors exist in the measurement method and in the interpretation of the resonance frequencies: Different peaks/resonators can be mixed. Some of the peaks are broad and diffuse, and it is not possible to determine an exact value for the resonance frequency. The frequency spectrum for one sample varies from measurement to measurement (when the sample is reinserted). The latter can be explained by e.g. air bubbles or debris on the resonators.

#### IV. CONCLUSIONS AND FUTURE WORK

Fragile diaphragm-based acoustic resonators have been coated with a biocompatible 12 nm thick anatase TiO<sub>2</sub> layer without failure. The frequency spectra are measured in water before and after coating. The resonance peaks can still be detected after coating with TiO<sub>2</sub>, but an increase in the

resonance frequencies of about 2 % is measured. The increase in the resonance frequencies is explained by a thicker diaphragm due to the TiO<sub>2</sub> film.

The purpose of the experiments reported here was to evaluate the influence from one type of biocompatible coating on diaphragm-based acoustic resonators designed for fish identification. This work is the first in a series of experiments mapping out biocompatible coatings and their effect on diaphragm-based devices. Coming *in vitro* tests aim at detecting the biological response to the acoustical resonators and to distinguish the bio-growth depending on the different types of coating. The effect on device characteristics and stability will also be further investigated.

#### REFERENCES

- [1] W. Voss, D. Gad, K. H. Mucke, and H. J. Christen, "Intrathecal baclofen treatment. A palliative procedure for severe spasticity and dystonia," *Monatsschrift Kinderheilkunde*, vol. 157, pp. 1128-1136, 2009.
- [2] P. J. Chen, D. C. Rodger, R. Agrawal, S. Saati, E. Meng, R. Varma, M. S. Humayun, and Y. C. Tai, "Implantable micromechanical parylene-based pressure sensors for unpowered intraocular pressure sensing," *Journal of Micromechanics and Microengineering*, vol. 17, pp. 1931-1938, 2007.
- [3] Clausen, "An implanted micro electro mechanical system for permanent measurement of human brain pressure," in *Faculty of Mathematics and Natural Science*, vol. PhD. Oslo: Univeristy of Oslo, 2006, pp. 131.
- [4] M. Frischholz, L. Sarmiento, M. Wenzel, K. Aquilina, R. Edwards, and H. B. Coakham, "Telemetric Implantable pressure sensor for short- and long-term monitoring of intracranial pressure," *2007 Annual International Conference of the Ieee Engineering in Medicine and Biology Society, Vols 1-16*, pp. 514-518, 2007.
- [5] U. Schnakenberg, C. Kruger, J. G. Pfeffer, W. Mokwa, G. V. Bogel, R. Gunther, and T. Schmitz-Rode, "Intravascular pressure monitoring system," *Sensors and Actuators a-Physical*, vol. 110, pp. 61-67, 2004.
- [6] CardioMEMS, "EndoSure® Wireless AAA Pressure Sensor," 2010.
- [7] N. Wisniewski, F. Moussy, and W. M. Reichert, "Characterization of implantable biosensor membrane biofouling," *Fresenius Journal of Analytical Chemistry*, vol. 366, pp. 611-621, 2000.
- [8] D. F. Williams, *The Williams dictionary of biomaterials*. Liverpool: Liverpool University Press, 1999.
- [9] K. C. Popat and T. A. Desai, "Poly(ethylene glycol) interfaces: an approach for enhanced performance of microfluidic systems," *Biosensors & Bioelectronics*, vol. 19, pp. 1037-1044, 2004.
- [10] G. Voskerjian, M. S. Shive, R. S. Shawgo, H. von Recum, J. M. Anderson, M. J. Cima, and R. Langer, "Biocompatibility and biofouling of MEMS drug delivery devices," *Biomaterials*, vol. 24, pp. 1959-1967, 2003.
- [11] S. Holm, J. Brungot, A. Ronnekleiv, L. Hoff, V. Jahr, and K. M. Kjolerbakken, "Acoustic passive integrated transponders for fish tagging and identification," *Aquacultural Engineering*, vol. 36, pp. 122-126, 2007.
- [12] A. Ronnekleiv, J. Brungot, D. Wang, R. Bernstein, V. Jahr, K. Kjolerbakken, L. Hoff, S. Holm, and Ieee, "Design of micromachined resonators for fish identification," in *2005 IEEE Ultrasonics Symposium, Vols 1-4, Ultrasonics Symposium*, 2005, pp. 641-644.
- [13] M. Geetha, A. K. Singh, R. Asokamani, and A. K. Gogia, "Ti based biomaterials, the ultimate choice for orthopaedic implants - A review," *Progress in Materials Science*, vol. 54, pp. 397-425, 2009.
- [14] M. C. Sunny and C. P. sharma, "Titanium - Protein interaction: Changes with oxide layer thickness," *Journal of Biomaterials applications*, vol. 6, pp. 89-98, 1991.
- [15] U. Diebold, "The surface science of titanium dioxide," *Surface Science Reports*, vol. 48, pp. 53-229, 2003.
- [16] S. D. Senturia, *Microsystem design*. Boston: Kluwer Academic, 2002.